COMPUTER-AIDED DESIGN & APPLICATIONS, 2017
VOL. 14, NO. 2, 193–205
http://dx.doi.org/10.1080/16864360.2016.1223431

Matched part-pair blending for 3D shape creation

Shungang Hua, Ang Xiong and Maodong Bai

Dalian University of Technology, China

ABSTRACT

We present an efficient and practical 3D shape creation algorithm based on the part matching and blending. Given two existing 3D shapes, part correspondences are found firstly by part matching, then two effective methods are investigated to blend the matched part-pair. The rapid one, which corresponds facets and vertices between matched part-pair, blends the coordinates of the corresponding vertices and generates new vertices to create the new part. And the elaborate one, which parameterizes the matched part-pair, combines their meshes and interpolates the vertices for part variation. Finally, all blended parts are rearranged by means of the topological relations in the given shapes to produce the integrated variations. Experimental results indicate that this algorithm is capable of implementing continuous and multipath shape variation as well as creating novel and plausible 3D shapes. This technique could allow for more efficient shape blending in the product innovation design and the animation industry.

KEYWORDS

Shape variation; part matching; part blending; re-linking; shape creation

1. Introduction

3D shape variation—the process of automatic 3D shape creation which is based on existing 3D shapes, can be carried out by altering the geometries and topological structures of parts within the shape. Given some existing well-organized 3D shapes, the novel and creative shapes could be generated via part reshuffling and blending as well as part growing and shrinking. 3D shape creation is widely used in the areas of industrial product design, innovative design, CAD, computer animation and virtual reality, etc. An excellent 3D shape variation method is expected to be capable of creating non-trivial and plausible 3D shapes and inspiring designers in their modeling and design activities.

In recent years, more attentions have been paid to 3D shape variation in computer graphics and animation communities. Finding novel and plausible variations of existing 3D shapes is an extremely challenging research topic. A variety of 3D shape variation algorithms have been proposed to create novel and plausible shapes. The representative one is to reshuffle, replace or recombine the pre-segmented parts from existing shapes. Additionally, altering the topology of the inputs is a brand-new trend in 3D shape creation. However, most of these algorithms focus on the structure-varied and topology-varied, with little attention to the surface details of the inputs.

Inspired by the ideas, this paper proposes a robust 3D shape creation methodology by part matching and blending, which aims to create a plausible variation appearance while maintaining the functional plausibility and the surface details. Given two mesh shapes, the arbitrary one is selected as the foundation, regarding as the original shape, and the other as reference, regarding as the reference shape. Then match the parts between the two shapes and create blended parts either by calculating and updating the part vertex coordinates of the original shape, or by part spherical parameterization and mesh combination. In terms of the connected relationship between parts of the original shape and the reference shape, the re-linking step is executed to produce integrated variations. Experiments demonstrate that final created shapes are functionally similar to the inputs and structurally transitional from the original shape to the reference one, while maintaining their surface details.

The contributions of this paper are as follows:

(i) Propose a rapid part blending approach for producing in-between parts, which transits from the original part to the reference part in geometry with different blending coefficients.
(ii) Investigate an elaborate blending technique to create the in-betweens by spherical parameterization of a single part and mesh combination.

CONTACT Ang Xiong xiongang@mail.dlut.edu.cn

(iii) Present a continuous shape variation algorithm for creating novel and plausible 3D shapes based on part matching, blending and re-linking, while preserving the functional plausibility and the input details simultaneously.

The rest of this paper is organized as follows. Section 2 introduces the related work of 3D shape variation briefly; section 3 is an overview of the shape variation algorithm; section 4 shows the part matching method between the two given shapes; section 5 describes the part blending algorithm in details; section 6 explains the part relinking; finally, experimental results and discussions are presented in Section 7.

2. Related work

Since the Digital Michelangelo Project [15] led by Marc Levoy ushered in a new era of digital geometry processing, 3D geometrical modeling theory and technology have achieved a great progress in recent years, especially on modeling from existing shapes. Modeling from existing shapes could be considered as a modeling method that generates new shapes by part reshuffling and blending, part growing and shrinking as well as mesh-based metamorphosing of existing shapes.

Part reshuffling is an approach to shape creation through part replacement or recombination from existing shapes which exists in extensive literature. Jain et al. [11] started with a part database including varieties of parts from existing shapes and considered some constraints, that were deduced by shape segmentation, contact analysis, and symmetry detection, to recombine the different parts from the part database. The smart algorithm is capable of composing various novel shapes that maintain the symmetry and adjacency structure of the given shapes. Han et al. [10] proposed a new style transfer method for shape creation. The concepts of style and content of 3D shapes are introduced for part segmentation, which is performed to analyzed shapes in a set. Then novel shapes are created by style transfer. Kalogerakis et al. [12] defined a generative model of component-based shape structure for shape creation. The compact representation could be used to suggest reshuffling parts. Chaudhuri et al. [7] raised a very similar algorithm. They defined a probabilistic shape structure representation to guide part replacement or recombination. Zheng et al. [26] presented an approach to part reshuffling based on certain symmetric functional arrangements, which are special arrangements among symmetrically related substructures and bear close relation to object functions. Xu et al. [25] introduced set evolution to 3D shape creation. The evolution algorithm generates inspiring shapes by means of keeping the population fit and diverse. To summarize, these shape variation methods based on part reshuffling, mainly focused on the principle of part replacement or recombination, and are able to create various and plausible 3D shape if the input shapes contain a lot of compatible shape structures . Unlike these works, this paper would implement part blending instead of part replacement or reshuffling for various shape appearance.

The mesh-based metamorphosis could create new shapes by changing the mesh information of the existing shapes. Kanai et al. [13] presented an efficient framework for genus-0 shape metamorphosis between two topologically equivalent mesh shapes. Their method requires users to partition meshes and control surface correspondences. Based on specified correspondences, metamorphosis of every polygonal region is implemented by interpolating the corresponding vertices between two mesh shapes. Obviously, the applicability of the variation algorithm is very limited. Gregory et al. [9] proposed a similar approach. Firstly, the user specifies a curve net. Then surface correspondences between each sub-mesh of two objects are established by using area-preserving mapping. Lastly, metamorphosis is generated based on local refinements of a curve net. Breen et al. [6] expressed the metamorphosis of two meshes as a process in which one shape deforms to maximize its similarity with the another. The objective function is incrementally optimized while deforming an implicit surface model. The deformable surface is represented as a level set of a densely sampled scalar function. Such level-set models have been shown to mimic conventional parametric deformable surface models by encoding surface movements as changes in the grayscale values of a volume data set. Thus, a well-founded mathematical structure leads to a set of procedures that describes how voxel values could be manipulated to create deformations are represented as a sequence of volumes. Their algorithms could produce some in-betweens from two topologically equivalent meshes. However, they are not suitable for the shapes which have complex structures or discrepant topologies. By contrast, our method would be applied to process more general shapes. Furthermore, little user intervention is required for the shape creation.

The work in this paper is closely related to the part blending and morphing from existing examples which is an approach to create a new shape through interpolating two given shapes. Morphing involves solving a correspondence problem and requires a blending operator. Finding correspondences on surfaces [5] is a difficult task. Blending becomes easier when chooses a suitable representation, such as distance fields [8], and achieves more natural results when maintaining as-rigid-as-possible deformations [2]. Alhashim et al. [3]

introduced an algorithm for generating novel 3D models via topology-varying shape blending. Their methods mainly focus on varying the topology of the inputs, and are devoted to producing series of topology-varying in-betweens. Fundamental topological operations include split and merge. Extracting the applicable skeleton needs to be preprocessed. And the shape surface is reconstructed by Poisson reconstruction [14] which is a statistics-based mesh reconstruction method. By comparison, our algorithm aims to create the plausible variation appearance while maintaining the functional plausibility and the surface details. Hence, the mesh combination blending is utilized to create the mesh surface which could retain the shape details.

3. Overview

This work is to generate variations from existing shapes and the main goal is to create the plausible shape appearance while maintaining the functional plausibility and the surface details of the inputs. Assuming that the shapes are pre-segmented into some meaningful parts, the algorithm firstly implements the part matching step across two shapes to get matched part-pairs. Then traversing each part in the original shape to execute the blending step with its matched part. Part blending step could produce a series of in-betweens with different blending coefficients, and it would reveal a cross-dissolve effect. After performing all parts creation, the blended parts are integrated into the novel shape by shifting them to their suitable locations respectively. Therefore, main steps of the methodology are as follows:

- **Preprocessing**: The available shapes are assumed to have been made a preliminary preprocessing, and the preprocessing includes shape size unitization, orientation normalization and part segmentation. Size unitization could be conducted accurately by adjusting the vertex. Through analyzing and aligning the principal components [1] of the shape point cloud information, shape orientation could also be normalized efficiently. In addition, many existing methods [22] could be used to segment parts. Though size unitization and part segmentation are critical, they are not the focuses of this paper. Thus, for some unmanageable shapes, their orientations would be aligned manually and then segment them into some meaningful parts. All the shapes used next are assumed to be preprocessed properly.
- **Part matching**: Hausdorff distance metric [24] is adopted to match parts across two shapes. The Hausdorff distance between point sets of parts could measure their similarity. The distances are calculated for all parts across the original and the reference shape. And by sorting these Hausdorff distances values in ascending order, the matched part-pairs would be attained. Through part matching, most parts are matched, but there exist unmatched parts probably.
- **Blending**: After part matching, the blending step would proceed by two means: (i) corresponding and interpolating the vertices from the matched part-pair, or (ii) parameterizing the matched part-pair spherically and combining their meshes. To ensure the diversity of blending result, the different blending coefficients could be taken, and it would also be feasible to blend all the parts or just a portion involved in the given shapes.
- **Re-linking**: This re-linking step could be considered as a process of part layout. The created parts by blending step differ from the original in geometry, size and location, thus the shape consisting of these parts directly may disconnect or overlap in structure. For yielding reasonable connection and topology, the blended parts are shifted to suitable positions according to their relationships of contact and connection in the original and the reference shape.

4. Part matching between two shapes

Through matching process, it is expected to establish the best part corresponding relationship between the two given shapes. As to two parts from different shapes, the Hausdorff distance between their point sets could measure their similarity.

The Hausdorff distance measures how far two non-empty compact subsets of a metric space are from each other. It defines the closeness of two sets. A bigger value of the distance indicates a bigger non-matching extent [19]. Therefore, the smaller the distance between two parts is, the more similar they are.

Let $X = \{x_1, x_2, \ldots, x_m\}$ and $Y = \{y_1, y_2, \ldots, y_n\}$ be two non-empty subsets of a metric space. Hausdorff distance from set X to Y is a maximin function, defined as:

$$h(X, Y) = \max_{x \in X} \left\{ \min_{y \in Y} \{\|x - y\|\} \right\} \tag{1}$$

Where x and y are elements of sets X and Y respectively, and $\|x - y\|$ is any metric between these elements. For simplicity, $\|x - y\|$ is taken as the Euclidian distance between x and y. Similarly, there is $h(Y, X)$ from set Y to set X. The two distances $h(X, Y)$ and $h(Y, X)$ are sometimes termed as the forward and backward Hausdorff distance of X to Y.

This paper uses a more general definition of Hausdorff distance, which is defined as:

$$dH(X, Y) = \max\{h(X, Y), h(Y, X)\} \tag{2}$$

Figure 1. Examples of part matching between two shapes. The matched part-pair are rendered with the same color and the unmatched with pale brown.

It defines the Hausdorff distance between X and Y. And it could be used to measure the closeness of two point sets [20, 21].

The parts between two shapes could be matched by using a greedy algorithm. For each part in the original shape, the Hausdorff distances to all parts within the reference shape are computed to form the distance set *HD_set*, and find out the minimal Hausdorff distance $HD_{\min}$. If $HD_{\min}$ is less than the similarity threshold θ, the two parts with the minimal distance are greedily regarded as matched and served as a matched part-pair. Then delete the elements related to the matched part-pair from the set *HD_set*. This process is repeated until $HD_{\min}$ is greater than θ or all parts of one shape are matched. If there are still unmatched parts, they would be considered as null correspondence. Fig. 1 shows some examples of part matching between two shapes.

5. Part blending

The shape variation algorithm is based on the original shape and guided by the reference shape. The numbers of the parts in the two shapes may be different. While matching part, not only one-to-one part correspondence exists, but also one-to-null correspondence may exist between the original and the reference shape. For the parts associated with one-to-null correspondence, a part shrinking operation could be achieved, but it may bring inharmonious part dimension. In order to avoid the inharmony, the parts should be simply retained in the variation so as to preserve the size coherence. For the parts with one-to-one correspondence, a part blending step between the matched part-pair would be carried out.

This paper will demonstrate two complementary methods to blending the matched part-pair: (i) part vertex correspondence and interpolation, and (ii) part spherical parameterization and mesh combination. Now the detailed introduction will be given to them respectively.

5.1. Blending parts by vertex correspondence

The first blending algorithm is a very rapid one. Firstly, it traverses every triangular facet of the part in the original shape, also called the original part, to find out the corresponding triangular facet of the matched part in the reference shape, also called the reference part in the following. Then the vertex correspondences between two corresponding triangular facets are searched by means of the vertex coordinates and position relationships. Thus, every vertex of the original part would correspond to a vertex set belonging to the reference part. Subsequently, the vertex and its corresponding vertex set are interpolated to generate a new 3D coordinate, which would be used to update the vertices of the original part. Finally, the variation based on the original part is created.

5.1.1. Triangular facet corresponding

Based on every triangular facet in the original part, triangular facet corresponding intends to find out the

unique corresponding triangular facet from the reference part. In order to accurately match triangular facets between the matched part-pair, the distance between two triangular facets should be measured quantifiably. For the triangular facet f_{orig} from the original part and f_{ref} from the reference part, the distance between them is defined as:

$$Dist(f_{orig}, f_{ref}) = |\boldsymbol{op} - \boldsymbol{o'p'}| \tag{3}$$

Where $\boldsymbol{op}$ denotes the vector from o, the centroid of the original part, to p, the centroid of the facet f_{orig}; and $\boldsymbol{o'p'}$ denotes the vector from o', the centroid of the reference part, to p', the centroid of the facet f_{ref}.

For every triangular facet f_{orig}, its corresponding facet f_{ref} could be found with minimum distance.

If there exist the same principal axis direction between the matched part-pair, according to the distance definition above, the triangular facets between the matched part-pair would be corresponded accurately. However, if the principal axis directions are different, the results would deviate from the expectation. As illustrated in Fig. 2, it is hoped to search the correspondences of facet f_1 (marked in red) and facet f_2 (marked in green), and expect that the facet f_1 corresponds to the facet f_1' while the facet f_2 to the facet f_2' subjectively. However, the facet f_1 and f_2 would both correspond to the facet f_1' in global coordinate system. The reason is that the principal axes of the matched part-pair are not aligned, and the calculating result would be $Dist(f_2, f_1') < Dist(f_2, f_2')$. In most situations, there are different principal axis directions between the matched part-pair, therefore, some preprocessing has to been implemented before matching facets.

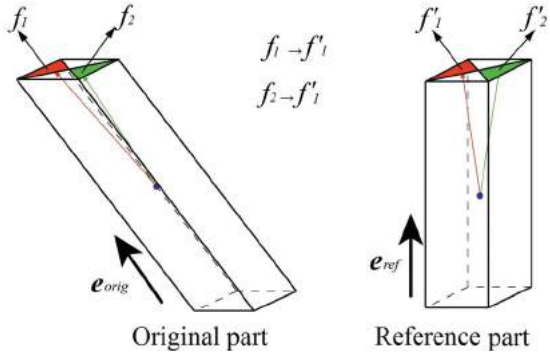

Figure 2. Corresponding triangular facets between the matched part-pair with different principal axis directions.

Hence, the principal axes of the matched part-pair are searched firstly and then aligned. The part principal axis could be calculated via Principal Component Analysis (PCA) [17], which is a statistical procedure that uses an orthogonal transformation to convert a set of observations of possibly correlated variables into a set of values of linearly uncorrelated variables called principal components. As is known to us, though PCA is an approximate way, it wonderfully suitable for the man-made shape which consists of regular and almost symmetrical parts. Using PCA to analyze the point cloud information of the part, their three principal components could be computed efficiently and accurately.

In general, the first principal component of the part is considered as its principal axis. However, if the first principal components of the matched part-pair vary dramatically, in this case, for the original part, its first principal component is considered as the principal axis; for the reference part, the principal component, which is closest to the principal axis of the original part, is served as its principal axis. Example is given by Fig. 3, in which the first principal component $\boldsymbol{e_1}$ of the original part is taken as its principal axis $\boldsymbol{e_{orig}}$. It's obvious that, for the reference part, the first principal component $\boldsymbol{e'_1}$ is quite different from $\boldsymbol{e_1}$ (namely $\boldsymbol{e_{orig}}$). Therefore, the principal component $\boldsymbol{e'_2}$, which is closest to $\boldsymbol{e_{orig}}$, is regarded as its principal axis $\boldsymbol{e_{ref}}$. By this means, the principal axes of the original and the reference part could be determined in accordance with their spatial locations.

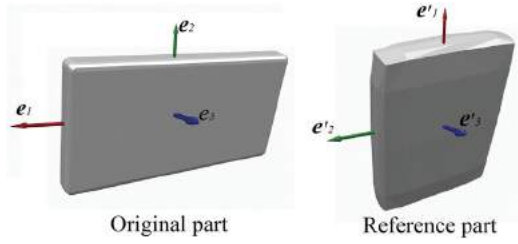

Figure 3. The first principal components of the original and the reference part are different greatly, so their first and second principal components are treated as their principal axes separately.

Next, the principal axes $\boldsymbol{e_{orig}}$ and $\boldsymbol{e_{ref}}$ of the matched part-pair would be aligned. The operation is implemented by rotating the vector $\boldsymbol{e_{orig}}$ and making it coincide with $\boldsymbol{e_{ref}}$ in a certain plane, which is decided by $\boldsymbol{e_{orig}}$ and $\boldsymbol{e_{ref}}$. In 3D coordinate system, the vector rotation could be achieved by a transformation matrix $\boldsymbol{M}$,

$$\begin{bmatrix} \boldsymbol{e_{orig}} \\ \dfrac{\boldsymbol{e_{orig}} \times \boldsymbol{e_{ref}}}{|\boldsymbol{e_{orig}} \times \boldsymbol{e_{ref}}|} \\ \dfrac{\boldsymbol{e_{orig}} \times \boldsymbol{e_{ref}} \times \boldsymbol{e_{orig}}}{|\boldsymbol{e_{orig}} \times \boldsymbol{e_{ref}} \times \boldsymbol{e_{orig}}|} \end{bmatrix} \boldsymbol{M} = \begin{bmatrix} \boldsymbol{e_{ref}} \\ \dfrac{\boldsymbol{e_{orig}} \times \boldsymbol{e_{ref}}}{|\boldsymbol{e_{orig}} \times \boldsymbol{e_{ref}}|} \\ \dfrac{\boldsymbol{e_{orig}} \times \boldsymbol{e_{ref}} \times \boldsymbol{e_{ref}}}{|\boldsymbol{e_{orig}} \times \boldsymbol{e_{ref}} \times \boldsymbol{e_{ref}}|} \end{bmatrix} \tag{4}$$

Here, the first matrix in Eqn. (4) is an orthogonal matrix, so:

$$\boldsymbol{M} = \begin{bmatrix} \boldsymbol{e_{orig}} \\ \dfrac{\boldsymbol{e_{orig}} \times \boldsymbol{e_{ref}}}{|\boldsymbol{e_{orig}} \times \boldsymbol{e_{ref}}|} \\ \dfrac{\boldsymbol{e_{orig}} \times \boldsymbol{e_{ref}} \times \boldsymbol{e_{orig}}}{|\boldsymbol{e_{orig}} \times \boldsymbol{e_{ref}} \times \boldsymbol{e_{orig}}|} \end{bmatrix}^{-1} \begin{bmatrix} \boldsymbol{e_{ref}} \\ \dfrac{\boldsymbol{e_{orig}} \times \boldsymbol{e_{ref}}}{|\boldsymbol{e_{orig}} \times \boldsymbol{e_{ref}}|} \\ \dfrac{\boldsymbol{e_{orig}} \times \boldsymbol{e_{ref}} \times \boldsymbol{e_{ref}}}{|\boldsymbol{e_{orig}} \times \boldsymbol{e_{ref}} \times \boldsymbol{e_{ref}}|} \end{bmatrix}$$
$$= \begin{bmatrix} \boldsymbol{e_{orig}} \\ \dfrac{\boldsymbol{e_{orig}} \times \boldsymbol{e_{ref}}}{|\boldsymbol{e_{orig}} \times \boldsymbol{e_{ref}}|} \\ \dfrac{\boldsymbol{e_{orig}} \times \boldsymbol{e_{ref}} \times \boldsymbol{e_{orig}}}{|\boldsymbol{e_{orig}} \times \boldsymbol{e_{ref}} \times \boldsymbol{e_{orig}}|} \end{bmatrix}^{\mathrm{T}} \begin{bmatrix} \boldsymbol{e_{ref}} \\ \dfrac{\boldsymbol{e_{orig}} \times \boldsymbol{e_{ref}}}{|\boldsymbol{e_{orig}} \times \boldsymbol{e_{ref}}|} \\ \dfrac{\boldsymbol{e_{orig}} \times \boldsymbol{e_{ref}} \times \boldsymbol{e_{ref}}}{|\boldsymbol{e_{orig}} \times \boldsymbol{e_{ref}} \times \boldsymbol{e_{ref}}|} \end{bmatrix} \tag{5}$$

After respecting their principal axes alignment, the distance between the triangular facets is rewritten as:

$$Dist(f_{orig}, f_{ref}) = |\boldsymbol{opM} - \boldsymbol{o'p'}| \tag{6}$$

5.1.2. Vertex corresponding

The moment triangular facets has corresponded, their vertices would be matched further. Firstly, the vectors from the centroids p and p' of triangular facets to their vertices are calculated respectively. Then, these vectors are mated in a clockwise direction, and the sums of the homologous vector differences could be obtained. Definitively, as shown in Fig. 4, the optimal vertex correspondence with the minimum sum would be found out.

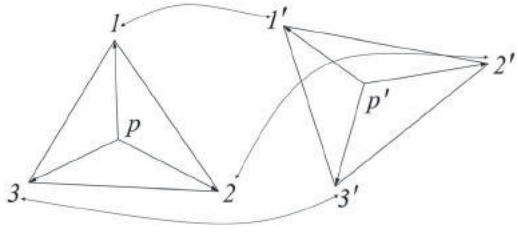

Figure 4. The vertex correspondences between the corresponding triangular facets.

After traversing all triangular facets of the original part to record the vertex correspondences, every vertex of original part finally corresponds to a vertex set belonging to the reference part. For a vertex v of original part, the new vertex v_{new} is generated by interpolating the vertex v and its corresponding vertex set $v_{set} = \{v_1, v_2, \cdots, v_m\}$,

$$v_{new} = k \times v_{ave} + (1 - k) \times v, \quad k \in [0, 1] \tag{7}$$

Where k is the blending coefficient, indicating the degree close to the reference shape in geometry. v_{ave} is the average value of the corresponding point set v_{set}, $v_{ave} = (v_1 + v_2 + \cdots + v_m)/m$.

At last, the blended part could be created with the interpolated vertices and the mesh structure of the original part. As shown in Fig. 5, while choosing different blending coefficient k, a continuous series of in-between parts would be generated.

5.2. Blending parts with spherical parameterization

In addition to the vertex correspondence blending method, in order to maintain the details adequately, the other elaborate blending technique by spherical parameterization [16] of a single part would be illustrated. The idea could be described as the following three steps: Firstly, normalizing the orientations and sizes of the matched part-pair. Secondly, producing the topological spheres M_o and M_r by parameterizing the matched part-pair onto a unit sphere, and combining them to create the combined topological spheres M_c. Thirdly, generating the blended parts via transforming the 3D vertex coordinates of M_c.

5.2.1. Part normalization

Actually, when it comes to part normalization, it implies the original vertex set V_o and the reference vertex set V_r are normalized for the matched part-pair. Once again, PCA is performed to calculate and align their principal axes, then, the transformed vertex sets $V'_o(V'_o = V_oM)$ and $V'_r(V'_r = V_r)$ could be acquired. After that, a scaling is provided by a diagonal 3×3 matrix S, $S = diag(s_x, s_y, s_z)$, which aims to transform the reference part so as to get the equal bounding box with the original part. More precisely, s_x, s_y and s_z describe the three edge length ratios of the original part bounding box and the reference one respectively.

5.2.2. Spherical parameterization and mesh combination

After the normalization, a spherical center projection method would be introduced for mapping the part onto a unit sphere, whose center is the part centroid. Moreover, if the centroid occurs outside the part, a local center which is closest to the part centroid would act as the unit sphere center. Even so, the foldovers often follow if the part contains complex surface details. Though some existing methods [18] could avoid that phenomenon, the method which relaxes the mapped topological spheres by Laplacian [23] iteration may be more straightforward and effective.

Laplacian is often described as a low pass filter, which could filter the high frequency. The discrete Laplacian of a discrete surface signal described by a function $x = \{x_1, x_2, \cdots, x_n\}^T$, could be defined by weighted averages

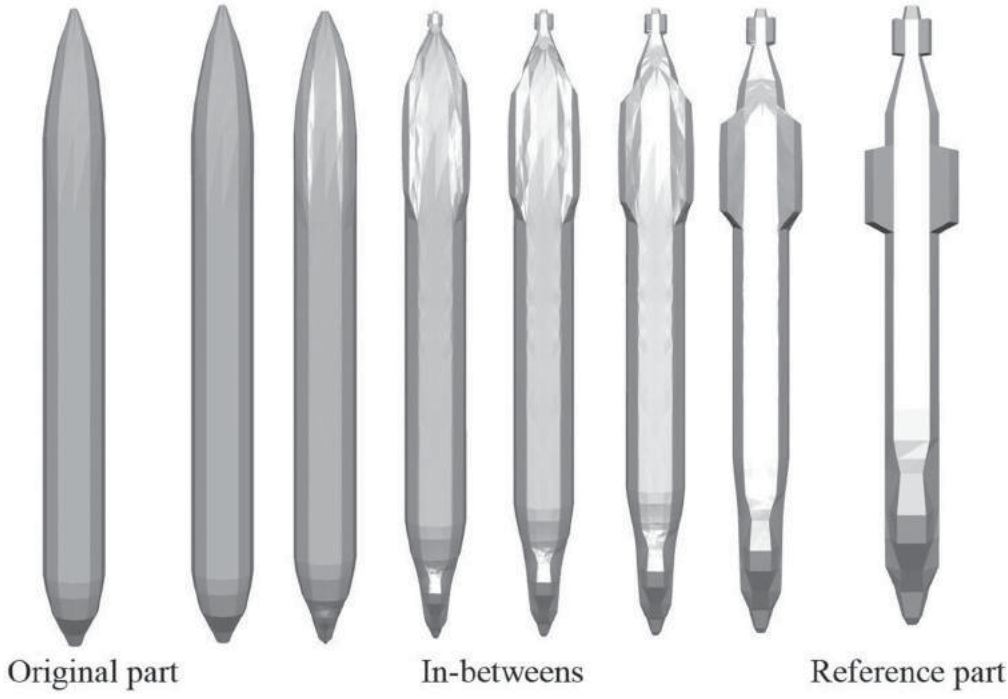

Figure 5. The blended results of plane body parts indicate that the blending algorithm is capable of producing a sequence of in-betweens with different blending coefficient *k*. *k* is 0, 0.2, 0.4, 0.6, 0.8, 1.0 from left to right sequentially.

over the neighborhoods,

$$L(x_i) = \Delta x_i = \sum_{j \in i^*} w_{i,j}(x_j - x_i), \quad i \in \{1, 2, \ldots, n\} \quad (8)$$

Where the set i^* is the neighbor vertex set of the vertex x_i, and the weights $w_{i,j}$ are positive numbers that add up to one, $\sum_{j \in i^*} w_{i,j} = 1$, for each i. Given different neighbouring structures, the weights could be chosen in various ways. One particularly simple and feasible choice is to set $w_{i,j}(\forall j \in i^*)$ equal to the inverse of the number of its neighbors.

The foldovers often occur on the sphere surface where the vertices are of the high frequency. So a low pass filter would be effective to eliminate the foldovers. Actually, with a uniform mesh, Laplacian iteration is a process that relaxes the sharp or high-frequency area and hardly change the even-distributed area. After mapping the part mesh onto a unit sphere surface, Laplacian iteration follows. If regarding the 3D vertex coordinates v_i as a vector signal, an iteration that relaxes the mesh with laplace operator could be described by:

$$V' = V + \Delta V = \{v_i' | v_i' = v_i + \Delta v_i, \Delta v_i = L(v_i)\} \quad (9)$$

In each iteration, to make sure all vertices lie on the unit sphere surface strictly, new generated vertex is supposed to be normalized, $v_i = v_i/|v_i|$. So far, the part has been mapped onto a unit sphere without foldovers, namely, the part has been parameterized spherically.

With the parametric topological spheres M_o and M_r of the original and the reference part, these following steps would be implemented to create the combined topological sphere M_c: (i) computing intersection points between M_o and M_r, (ii) systemizing the edges and vertices on the basis of the intersection, (iii) traversing each edge and creating clockwise edge cycles to generate faces, and (iv) triangulating all the generated faces to form the final combined mesh M_c. The process is illustrated in Fig. 6.

5.2.3. Blending

Through the previous subsection, the original and the reference part could be represented respectively in single, another mesh structure of M_c. And from a high-level view, part blending could be understood as the process of endowing the vertices of M_c with different 3D coordinates. While the vertices of M_c could be classified into three categories: (i) vertices from M_o mapped by V_o, (ii) vertices from M_r mapped by V_r, and (iii) intersection vertices between M_o and M_r on the unit sphere surface. With the purpose of blending parts on basis of the mesh structure of M_c, each of its vertices must be taken into account and determined. In this end, it is imperative to investigate the 3D coordinates V_{c-o} and V_{c-r} respectively when the original and the reference part are represented

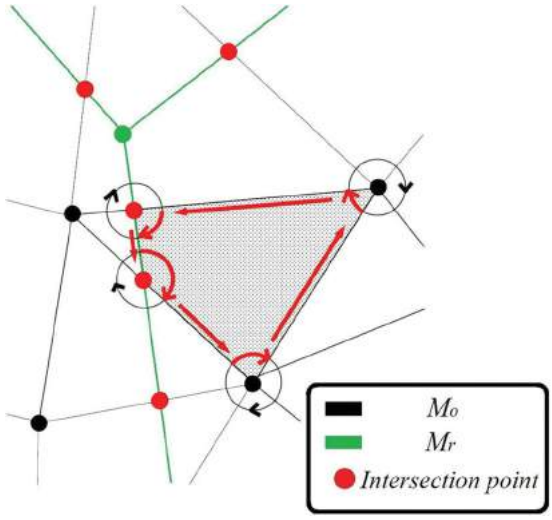

Figure 6. Facet is created along edge cycles in M_c.

with the mesh structure of M_c. Here, computing V_{c-o} is illustrated to demonstrate the process. For those vertices from M_o, their 3D coordinates are defined as the original positions in the original part, namely, V_o. As for every vertex in M_r, it must be involved in a certain triangle facet of M_o. In terms of their relative locations from every certain triangle facet, their barycentric coordinates in every certain triangle facet of M_o would be calculated, finally, every vertex in M_r could be denoted with triangle vertices involved in V_o. And for the intersection vertices, each of them must be on a certain edge of M_o and could be obtained according to the original edge vertices involved in V_o. Fig. 7 illustrates the process. Similarly, V_{c-r} could be obtained.

The entire one-to-one vertex correspondences exist between V_{c-o} and V_{c-r}. Fig. 8 shows V_{c-o} and V_{c-r} could generate the original and the reference part respectively with the mesh structure of M_c. And further, by interpolating vertex positions from V_{c-o} and V_{c-r}, the generated part gradually transforms from the original part to the reference. For the blending coefficient $k(0 < k < 1)$, the blended vertices could be computed as follows:

$$V_c(k) = kV_{c-o} + (1-k)V_{c-r} \tag{10}$$

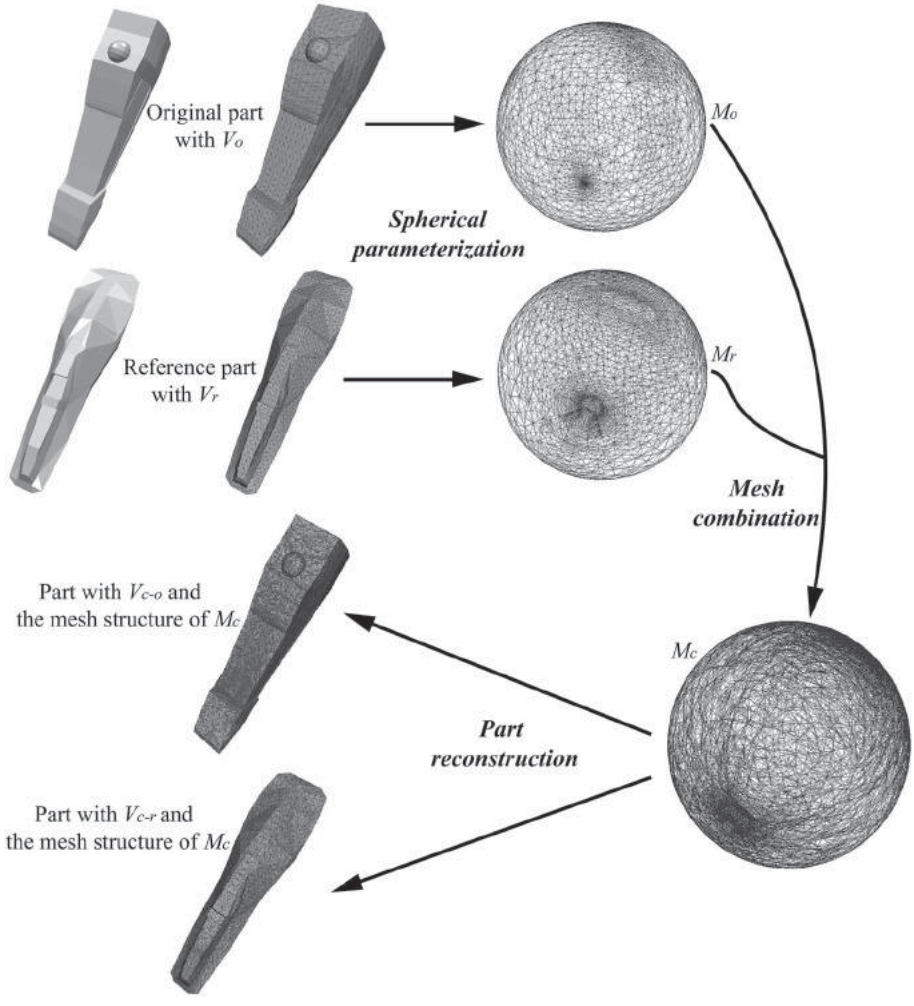

Figure 7. The process of spherical parameterization, mesh combination and part reconstruction.

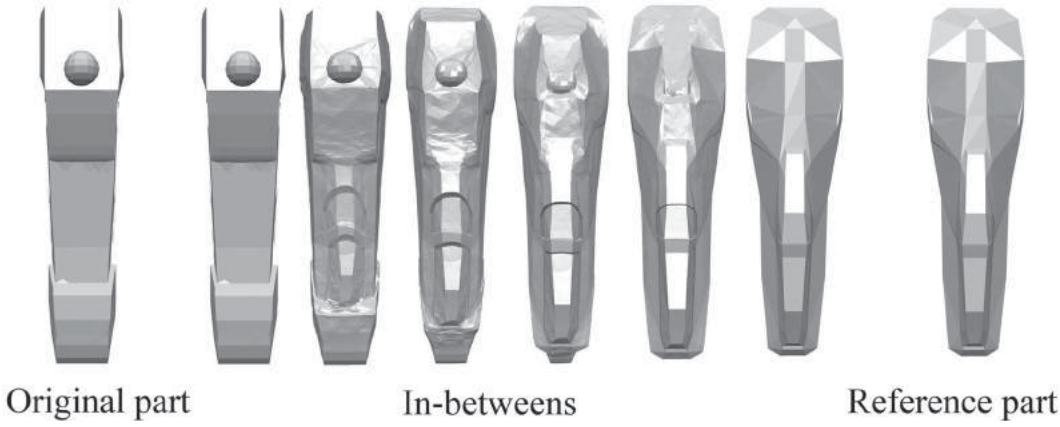

Figure 8. With different blending coefficient k, the blending part changes gradually from the original part to the reference one. Here k is 0, 0.2, 0.4, 0.6, 0.8, 1.0 from left to right sequentially.

6. Part re-linking

Although preserving the pristine vertex topological relations, obviously, the blended parts vary markedly in their meshes from the original parts. Thus, they would be different from the original ones in geometry, dimension and position. If the variation shape is directly composed of these parts, the part disconnection and overlap would probably occur. And these examples are shown in Fig. 9(a). To ensure connection and topology plausibility of the variation, a part re-linking step is supposed to be implemented.

In terms of part contact and connection in the original shape, the blended parts would be suitably laid out by part re-linking. To start with, a certain part is chosen as the basic part, which usually is the maximum in geometry dimension, or locates in the middlemost of the original shape. Then the positions of all other parts relative to the basic part could be acquired. Actually, the nearest vertex sets of the two parts are recorded as their connection.

If two parts of the original shape have the connection $c_1 = (S_1, S_2)$, namely, S_1 and S_2 are the nearest vertex sets across the two parts. And the corresponding connection $c_2 = (S_1', S_2')$ of their respective matched parts from the reference shape could be gained similarly. With the blending coefficient k, the corresponding connection $c_b(k)$ of the blended parts could be calculated, $c_b(k) = kc_1 + (1 - k)c_2$. As shown in Fig. 9(b), the integrated and plausible variations would be formed after adjusting the blended parts to maintain their calculated connections.

7. Experiment and discussion

In order to verify the effectiveness and practicability of this methodology, this paper collects a lot of 3D mesh shapes, such as chair, table, and plane, etc., from the Internet and literature [3, 4] for variation creation. These shapes have been preliminarily preprocessed such as shape size and orientation normalization, part segmentation. Two different blending algorithms are implemented respectively, Figs 10 and 11 show the main results.

The below variation sequences shown in Fig. 10 are created through the first blending method. The leftmost are the original shapes and the rightmost are the reference shapes. The four in-betweens are created with blending coefficient 0.2, 0.4, 0.6, 0.8 respectively. For two given shapes, the blending results are different when taking the alternative original shape, and the examples are shown in

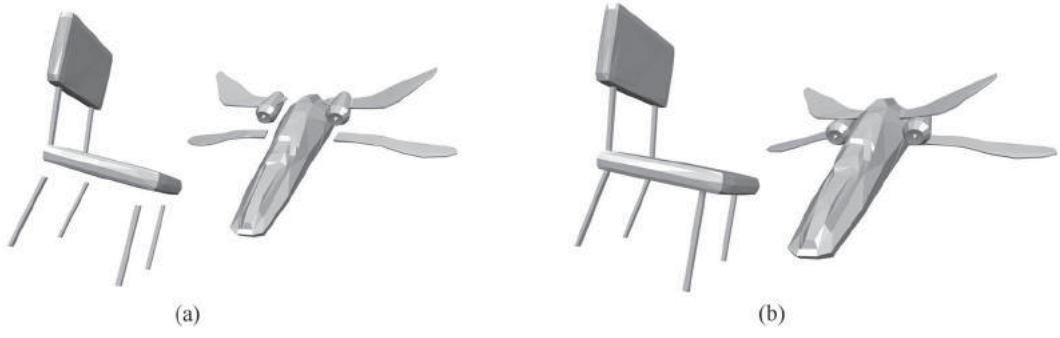

Figure 9. (a) Part disconnection and overlap in the shape, which is composed of the blended parts directly, (b) Examples of plausible shapes integrated after re-linking parts.

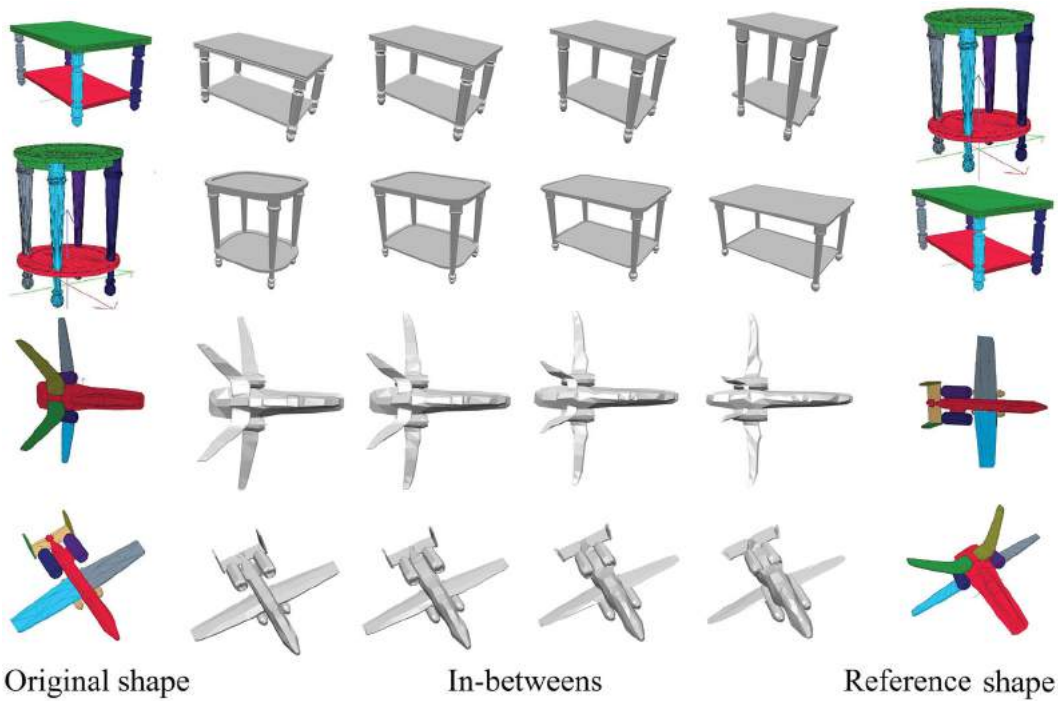

Figure 10. Blending results of some shapes in the first blending approach.

Fig. 10 (See Row 1 and 2, Row 3 and 4). The blending coefficient k could take a value from 0 to 1, which means the reference shape accounts for a gradually increasing percent age while the original shape accounts for a gradually decreasing percent age in geometry. And as the coefficient k increases, the in-betweens transit from the original shape to the reference one in geometry. It could be observed that the general features of the variations depend on the original shape, while the detail features are determined by both the original and the reference shape. The new shapes vary in geometry, but maintain the topology of the original shape. Thus, the functional plausibility of the original shape would be kept. (Note that the table tops of the betweens in Row 1 keep cubiform because the top of the original shape is concise and only includes some peak vertices. And if k is equal to 0, some foldovers would occur. Consequently, the blending method is unsuitable for thorough variation.)

In the process of vertex corresponding, experiments are made to compute correspondences on vertices directly rather than on facets. At the same time, employing the manner of the vector direction difference instead of the previous vector difference to define the correspondence distance. However, the experiments show that these alteration would often introduce some mesh foldovers and holes, and the original algorithm is more resilient to create plausible variations. In addition, as for the spindly part, segmenting it firstly and then executing the triangular facet and vertex corresponding for each segments could improve the precision.

Fig. 11 shows some typical blending examples in the second blending approach. For each row, the blending coefficient k is 0, 0.2, 0.4, 0.6, 0.8, 1.0 from left to right respectively. Given two shapes, if all of their parts are of the one-to-one part correspondence, the method would generate the same variation results when taking the alternative original shape, and the variation could change thoroughly from the original shape to the reference one. This has been fully borne out by the sequences in Row 1, 2, 3, 4, 5, 8 and 10. Almost inevitably, if part with one-to-null correspondence exists between the two given shapes, just retaining them. Specifically, as the variations shown in Row 6, 7, 9, 11, 12 and 13, the one-to-null parts from the original shape are kept in the variations with the blending coefficient $0 \sim 0.5$, and those from the reference are retained in the variations with the blending coefficient $0.6 \sim 1.0$.

As Laplacian iteration is applied to eliminate the foldovers, so the blending process is more elaborate but more time-consuming. Experiments discover that the iteration is not always effective to thoroughly estimate the foldovers. As little slight foldovers would not do matter in the blending results, so iterating 50 times would be chosen strategically as one of the termination conditions. And the variation sequences in Figs 10 and 11 show that the in-betweens maintain more details in the second method and undergo a more thorough variation.

Moreover, the variation could also be generated by blending an appointed portion of matched part-pairs. Fig. 12 just blends the top and the bottom board of the

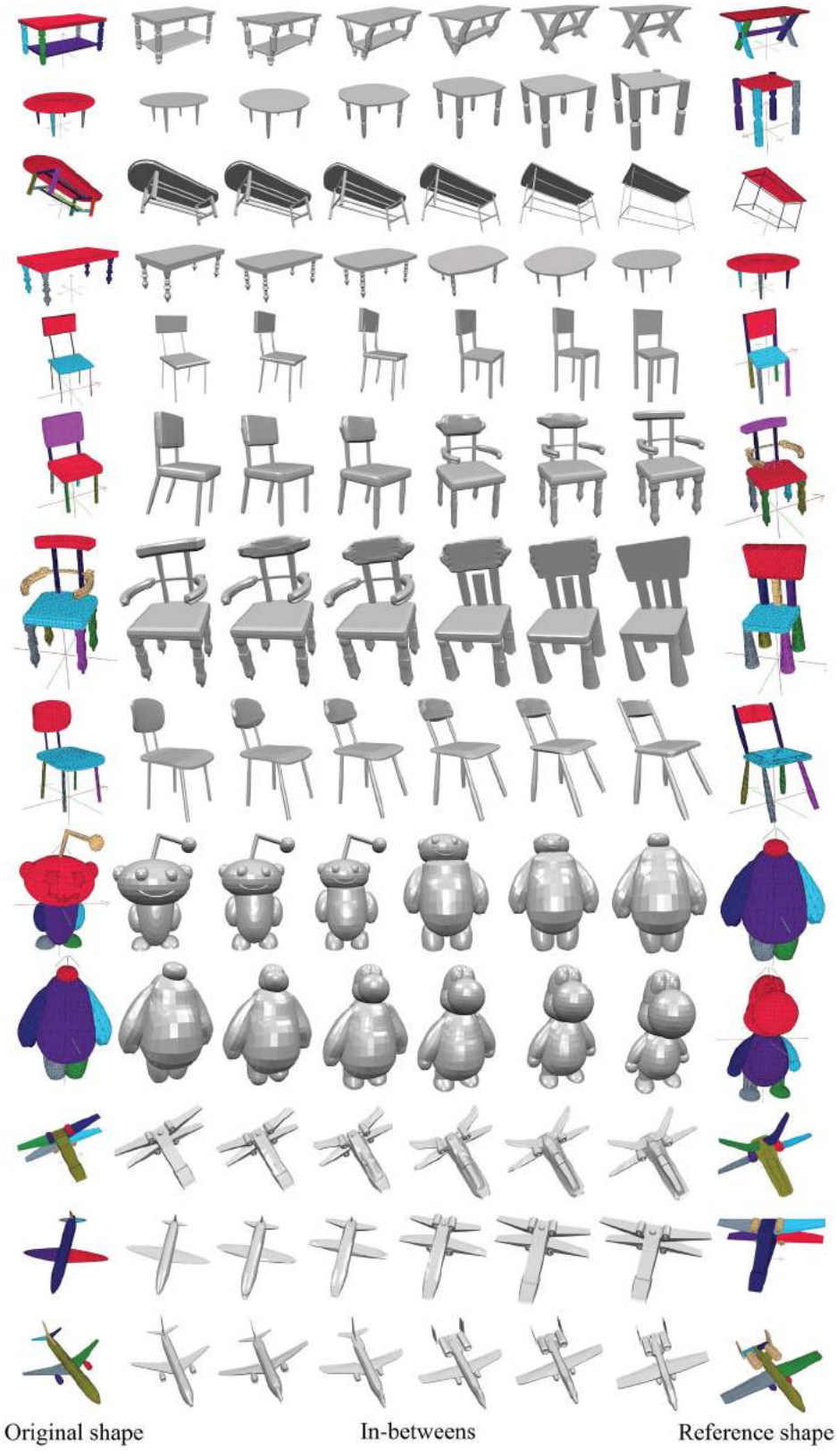

Figure 11. Variation sequences with sequential blending coefficients in the second blending approach.

two tables. If the densities of the point clouds of two given shapes are high and approximate, the algorithm serves as the method of part replacement or recombination while the coefficient k is equal to 1. Through selectively blending the matched part-pairs, the diversities of the variations could be expanded as well.

In the present paper, the input shapes include chair, table, plane, and doll, etc. These shapes have been

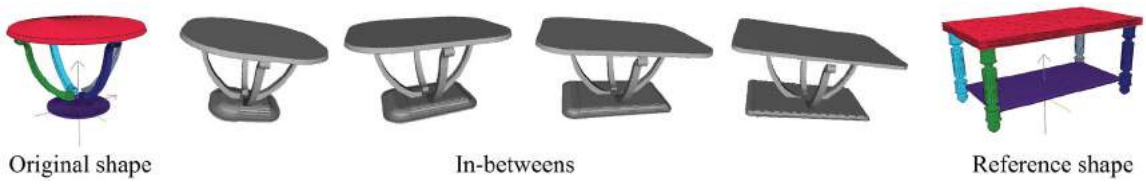

Figure 12. A variation sequence by blending a portion of matched part-pairs. *k* is 0.2,0.4,0.6,0.8 respectively for in-betweens.

preliminarily preprocessed such as shape size and orientation normalization, part segmentation. After segmentation, the numbers of parts in the models range from 2 to 15, their vertex numbers per part range from 8 to 1000 that is sufficient for a reasonable level of details. The algorithm is implemented on an Intel Core i5 3.20 GHz desktop PC with 4GB memory. Its computational complexity depends on the geometric complexity and the vertex number of the inputs.

Further, the shape preprocessing time mainly depends on its complexity. Some models need to be segmented manually if they come without appropriate segmentation. It would take several minutes to preprocess a typical model. The experimental results show that, after shape preprocessing, it takes less than 2 sec to generate a variation sequence from the input-pair by the first method, and about 4 min in average by the second one. For the plane shapes shown in Fig. 10 Row 3, the original and the reference shape contain 7 and 11 parts respectively; their average vertex numbers per part are about 710 and 560. To generate a variation sequence, the first method requires 970 ms, which contains 90 ms part matching time, 630 ms part blending time and 70 ms part re-linking time; yet the second method would take 170 sec that contains 110 ms part matching time, 170 sec part blending time and 190 ms part re-linking time. As a note, if the average vertex number per part of the input exceeds 2000, the blending time by the second algorithm would increase heavily.

According to the uniqueness of each blending algorithm, the alternative methods could fit for the need of various occasions. More specifically, the first one could satisfy real-time field, while the second one could create more elaborate variations.

Though the methodology could create rich variations, there still exist some limitations. The created variation is similar to the inputs in geometry and functionality, such that, any scalable 3D shape beyond the zone and scale of the two inputs could be generated hardly. Besides, in the algorithm, every triangular facet and vertex would be handled to generate the new meshes based on the given meshes, so the well-meshed shapes are required as the inputs. If the input part is not the genus-0 mesh or includes some defects such as mesh foldovers and hole, the algorithm may magnify the defect or even fail. Hence, the man-made shapes with well-organized mesh would be the optimal input choice.

In comparison to topology-varying of Ibraheem Alhashim et al. [3], which focuses on varying the topology of the inputs, our method aims to create the plausible 3D shape appearance by part matching and blending. In topology-varying, a lot of 3D models are created undergoing topology variation. However, most of them are implausible in functionality and structure. And a few of clearly implausible in-betweens could be removed via preserving part symmetry and connection. While our methodology retains the topological structures of the inputs to maintain the functional plausibility. The variation process is a transition from the original shape to the reference one, and could create a series of similar plausible shapes with no need for implausibility filter. Besides, the Poisson reconstruction is used by them to construct the coarse mesh; by contrast, our algorithm utilizes a mesh combination blending to create the mesh surface, which could retain the shape details. As illustrated in Fig. 11, the surface texture of the original table legs in Row 1, 2 and 4 is inherited well in their variations, as is the doll head feature in Row 9 and 10.

8. Conclusion

Based on part matching and blending of the existing shapes, an efficient and novel 3D shape creation algorithm is proposed. The algorithm firstly conducts part matching by Hausdorff distance metric, then raises two complementary means to blend the matched part-pair. In the first approach, the triangular facets and vertices are corresponded, and the in-between parts are created by interpolating the corresponding vertices. While in the second one, the part-pair are parameterized spherically to a combined mesh, and the in-between parts are produced by interpolating the vertex of the combined mesh. Finally, the in-betweens are re-linked to create a series of variations. The algorithm mentioned above could blend a portion or all of the matched part-pairs and implement continuous multipath shape variation. The generated variations are of the plausible shape appearance and functionality, and retain the adequate details

of the inputs. On the basis of the matched part-pair blending as well as part replacement, a utility tool is developed for 3D shape creation.

In the variation creation, it is difficult to keep balance between retaining details and saving time. Besides, the current method mainly focuses on the appearance of the variation, while its mesh quality is ignored. Hence, a new method, which is capable of efficiently creating multifarious variations with excellent mesh quality and maintaining the indispensable details of the inputs, will be given a further exploration.

ORCID

Ang Xiong http://orcid.org/0000-0002-2213-4726

References

[1] Abdi, H.; Williams, L. J.: Principal component analysis, Wiley Interdisciplinary Reviews: Computational Statistics, 2(14), 2010, 433–459. http://dx.doi.org/10.1002/wics.101

[2] Alexa, M.; Cohen-Or, D.; Levin, D.: As-rigid-as-possible shape interpolation, In: Proceedings of ACM SIGGRAPH, 2000, 157–164. http://dx.doi.org/10.1145/344779.344859

[3] Alhashim, I.; Li, H. H.: Topology-Varying 3D Shape Creation via Structural Blending, ACM Trans Graphics, 33(4), 2014, 1–10, Article No. 158. http://dx.doi.org/10.1145/2601097.2601102

[4] Alhashim, I.; Xu, K.; Zhuang, Y.; et al.: Deformation-driven topology-varying 3D shape correspondence, ACM Transactions on Graphics, 34(6), 2015, 1–13. http://dx.doi.org/10.1145/2816795.2818088

[5] Beier, T.; Neely, S.: Feature-based image metamorphosis, Computer Graphics, 26(2), 1992, 35–42. http://dx.doi.org/10.1145/142920.134003

[6] Breen, D. E.; Whitaker, R. T.: A level-set approach for the metamorphosis of solid models, IEEE Transactions on Visualization and Computer Graphics, 7(2), 2001, 173–192. http://dx.doi.org/10.1145/311625.312113

[7] Chaudhuri, S.; Kalogerakis, E.; Guibas, L.; Koltun, V.: Probabilistic reasoning for assembly-based 3D modeling, ACM Trans Graphics, 30(4), 2011, 1–10, Article No. 35. http://dx.doi.org/10.1145/2010324.1964930

[8] Cohen-Or, D.; Solomovic, A.; Levin, D.: Three-dimensional distance field metamorphosis, ACM Trans Graphics, 17(2), 1998, 116–141. http://dx.doi.org/10.1145/274363.274366

[9] Gregory, A.; State, A.; Lin, M.; Manocha, D.; Livingston, M.: Feature-based surface decomposition for correspondence and morphing between polyhedra, In: Proceedings of Computer Animation, 1998, 64–71. http://dx.doi.org/10.1109/CA.1998.681909

[10] Han, Z.; Liu, Z.; Han, J.; et al.: 3D shape creation by style transfer, Visual Computer International Journal of Computer Graphics, 31(9), 2015, 1147–1161. http://dx.doi.org/10.1007/s00371-014-0999-1

[11] Jain, A.; Thormählen, T.: Exploring Shape Variations by 3D-Model Decomposition and Part-based Recombination, Computer Graphics Forum, 31(2), 2012, 631–640. http://dx.doi.org/10.1111/j.1467-8659.2012.03042.x

[12] Kalogerakis, E.; Chaudhuri, S.: A probabilistic model for component-based shape synthesis, ACM Trans Graphics, 31(4), 2012, 1–11, Article No. 55. http://dx.doi.org/10.1145/2185520.2185551

[13] Kanai, T.; Suzuki, H.; Kimura, F.: Metamorphosis of arbitrary triangular meshes, IEE Computer Graphics & Applications, 20(2), 2000, 62–75. http://dx.doi.org/10.1109/38.824544

[14] Kazhdan, M.; Bolitho, M.; Hoppe, H.: Poisson surface reconstruction, In: Proceedings of the fourth Eurographics Symposium on Geome-try Processing; 2006, 61–70. http://dx.doi.org/10.2312/SGP/SGP06/061-070

[15] Levoy, M.; Pulli, K.; Curless, B.; Rusinkiewicz, S.; Koller, D.; Pereira, L.; Ginzton, M.; Anderson, S.; Davis, J.; Ginsberg, J.; Shade, J.; Fulk, D.: The Digital Michelangelo Project: 3D Scanning of Large Statues, In: Proceedings of ACM SIGGRAPH, 2000, 131–144. http://dx.doi.org/10.1145/344779.344849

[16] Alexa, M.: Recent Advances in Mesh Morphing, Computer Graphics Forum, 21(2), 2002, 173–198. http://dx.doi.org/10.1111/1467-8659.00575

[17] Papadakis, P.; Pratikakis, I.; Perantonis, S.; Theoharis, T.: Efficient 3D shape matching and retrieval using a concrete radialized spherical projection representation, Pattern Recognition, 40(9), 2007, 2437–2452. http://dx.doi.org/10.1016/j.patcog.2006.12.026

[18] Praun, E.; Hoppe, H.: Spherical parametrization and remeshing, ACM Transactions on Graphics, 22(3), 2003, 340–349. http://dx.doi.org/10.1145/882262.882274

[19] Rockafellar, T. R.; Wets, R. J. B.: Variational Analysis, Springer-Verlag Berlin Heidelberg, Berlin, 2005, 117. ISBN 3540627723. http://dx.doi.org/10.1007/978-3-642-02431-3

[20] Rote, G.: Computing the minimum Hausdorff distance between two point sets on a line under translation, Information Processing Letters, 38(3), 1991, 123–127. http://dx.doi.org/10.1016/0020-0190(91)90233-8

[21] Rucklidge, W.: Efficient computation of the minimum Hausdorff distance for visual recognition, Ph.D. thesis, Dept. of computer science, Cornell University, NY, 1995. http://dl.acm.org/citation.cfm?id = 239404

[22] Shamir, A.: A survey on Mesh Segmentation Techniques, Computer Graphics Forum, 27(6), 2008, 1539–1556. http://dx.doi.org/10.1111/j.1467-8659.2007.01103.x

[23] Taubin, G.: A Signal Processing Approach to Fair Surface Design, In: Conference on Computer Graphics & Interactive Techniques. 1999, 351–358. http://dx.doi.org/10.1145/218380.218473

[24] Wikipedia: Hausdorff distance; 2015. https://en.wikipedia.org/wiki/Hausdorff_distance

[25] Xu, K.; Zhang, H.: Fit and diverse: Set evolution for inspiring 3d shape galleries, ACM Trans Graphics, 31(4), 2012, 1–10, Article No. 57. http://dx.doi.org/10.1145/2185520.2185553

[26] Zheng, Y. Y.; Cohen-Or, D.: Smart Variations: Functional Substructures for Part Compatibility, Computer Gr Forum, 32(2), 2013, 195–204. http://dx.doi.org/10.1111/cgf.12039